

## Time-Resolved X-ray diffraction Investigation of Austenite and Transformation to Bainite<sup>†</sup>

S. S. Babu<sup>1</sup>, E. D. Specht,<sup>2</sup> S. A. David,<sup>2</sup> E. Karapetrova,<sup>3</sup> P. Zschack,<sup>3</sup>  
M. Peet<sup>4</sup> and H. K. D. H. Bhadeshia<sup>4</sup>

<sup>1</sup>Edison Welding Institute, 1250 Arthur Adams Drive, Columbus, Ohio, 43221, USA

<sup>2</sup>Materials Science and Technology Division, Oak Ridge, TN 37831, USA

<sup>3</sup>Frederick Seitz Materials Research Laboratory, University of Illinois at Urbana-Champaign, Illinois 61801, USA

<sup>4</sup>Materials Science and Metallurgy, University of Cambridge, Cambridge, CB23QZ, UK

**Abstract:** In-situ time-resolved X-ray diffraction technique with synchrotron radiation was used to track austenite decomposition in steels. Measurements from a Fe-C-Si-Mn steel indicate two lattice parameters in the austenite, possibly due to the development of carbon-rich and carbon-poor austenite prior to transformation. The lattice parameter became uniform with the progress of transformation and the fraction of carbon-poor austenite decreased. The bainitic ferrite itself exhibited a range of lattice parameters during the early stages of transformation, due to the trapping of carbon. The results are in agreement with atom probe data. In order to evaluate the generality of this phenomenon, the experiments were repeated in Fe-Ni and Fe-Ni-C steels. Preliminary evidence shows the tendency for the development of austenite peak splitting even in Fe-Ni-C alloys.

### 1. INTRODUCTION

A new class of steels, based on Fe-C-Si-Mn system, with high-strength (2500 MPa) and high toughness (30 MPa m<sup>1/2</sup>) has been developed [1]. The microstructure consists of 20-40 nm sized bainitic ferrite plates, which are partially supersaturated with carbon and retained austenite with a volume fraction in the range 0.2-0.4. This microstructure can be generated at low cost, without severe heat-treatments and in samples, which are large in all three dimensions. Silicon is used to suppress cementite precipitation during the bainite transformation, which occurs at remarkably low temperatures in the range 473--573 K [2, 3].

Previous work [4] indicated a peculiar and ill-understood phenomenon in which the austenite, prior to its transformation, appears to develop regions with two different lattice parameters. The purpose of the present work was to design specific experiments to further elucidate this phenomenon using carbon-free and carbon-containing austenites in the Fe-Ni-C system.

### 2. EXPERIMENTATION

#### 2.1 Alloys

The compositions of the steels studied are in Table 1. Rectangular rod samples 2 × 4 × 95 mm were machined from large bars. These rods were homogenized in an argon-filled quartz tubes at 1473 K for 48 h, followed by quenching in water to generate a mixture of martensite and retained austenite.

Table 1. Composition of the steels (in wt %) used in this investigation

Alloy	C	Si	Mn	Ni	Cr	Mo	V	Al	P	S
FeCSiMn	0.75	1.63	1.95	-	1.48	0.29	0.1	0.01	0.003	0.003
FeNi	0.007	1.78	0.01	14.94	0.32	0.01	-	0.03	0.023	0.003
FeNiC	0.34	1.82	0.01	15.11	0.31	0.01	-	0.01	0.023	0.003

#### 2.2 X-ray Analysis

These experiments were conducted on a synchrotron X-ray beam line X33-BM at the Advanced Photon Source in Argonne, Illinois – the details are in [4]. A double-crystal Si(111) monochromator selected and sagittally focused 30 keV X-rays, with a penetration depth in steel of 0.16 mm. Slits defined a beam 0.25 mm high and 1.0 mm wide on the sample. A schematic illustration of the experiment and a typical diffraction image is shown in Fig. 1. The minimum time resolution that can be attained in this set up without deterioration of signal to noise ratio was found to be 3 s. The samples were heated to 1273 K and held at that temperature for 4 min. Then the steel was cooled at a rate of 10 K s<sup>-1</sup> from 1273 K to 573 K and held at that temperature for different time periods. The temperature was controlled using direct resistive-heating using a type-S (Pt/Pt10%Rh) thermocouple. Oxidation was reduced by covering the sample with an inverted can filled with He.

<sup>†</sup> The submitted abstract has been authored by a contractor of the U.S. Government under contract DE-AC05-00OR22725. Accordingly, the U.S. Government retains a nonexclusive, royalty-free license to publish or reproduce the published form of this contribution, or allow others to do so, for U.S. Government purposes.

### 3. RESULTS

#### 3.1 Results from FeCSiMn steel

Typical diffraction data, obtained during isothermal heat treatment at 573 K, as a function of time are shown in Fig. 2. The blue colour corresponds to the background intensity and red represents the maximum intensity. In the early stages of heat treatment only diffraction peaks corresponding to the face-centred cubic (FCC) austenite crystal structure were observed. With continued holding and prior to transformation, the FCC  $\{111\}$ -peak broadened and after a particular time the peak profile became bimodal as indicated by *A* in Fig. 2. This was also the case for  $\{002\}$  peaks [C in Fig. 2].

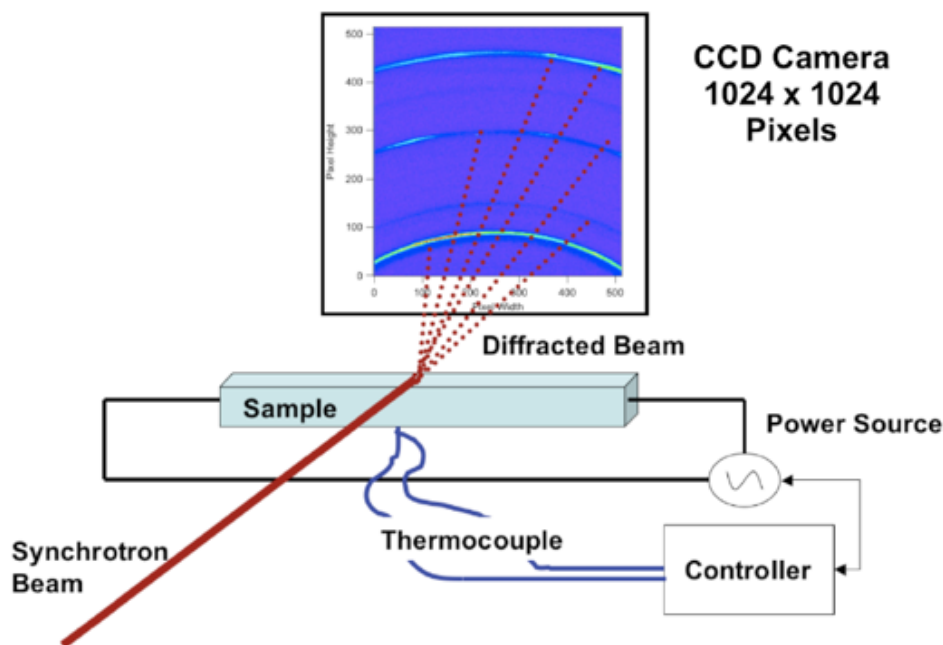


Fig.1 Experimental arrangement for time-resolved X-ray diffraction investigation using synchrotron beam line

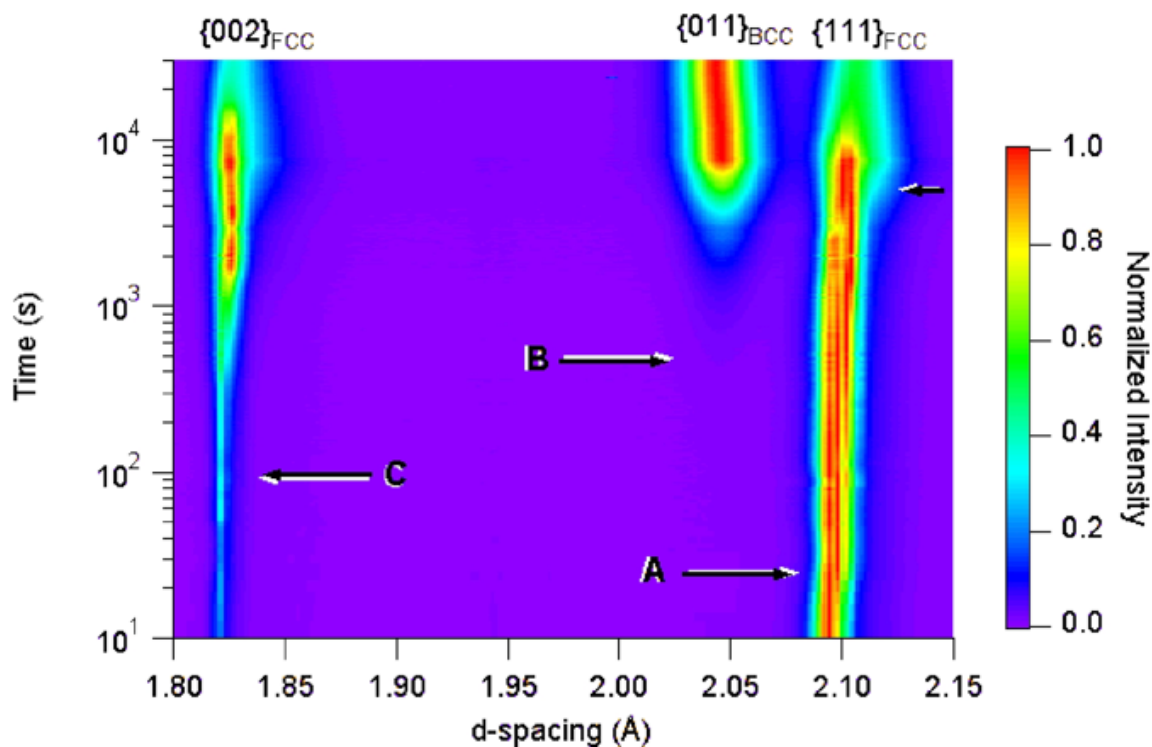


Fig.2 X-ray diffraction data from FeCSiMn steel during isothermal transformation at 573 K in an image format

After isothermal holding for more than 500 s, faint peaks corresponding to the body-centred cubic (BCC) crystal structure of ferrite marked the beginning of the bainite reaction, *B* in Fig. 2. The BCC intensity then increased and the

austenite peaks became more uniform with its lattice parameter expanding due to enrichment with carbon partitioned from the bainitic ferrite. The ferrite lattice parameters corresponded to about 0.4 to 0.62 wt% carbon [4], consistent with atom probe measurements (0.03 to 0.5 wt. %C) [2].

The broadening and development of a bimodal profile in the austenite diffraction peaks is not properly understood [4]. It may not be appropriate to regard the {111} data as a single peak, but rather due to the superposition of two austenite peaks corresponding to different lattice parameters. This is referred to here as “peak splitting” as might occur if carbon-rich and carbon-poor regions develop spontaneously. The deconvolution of the data in Fig. 2 was done using a Gaussian shape and some representative analyses are provided in Fig. 3. The results illustrate peak-splitting as soon as the sample reaches 573 K and at 100 s. From previous observations [4] the intensity of the low  $d_{111}$  peak decreases as ferrite develops. This result is consistent with the elimination of low-carbon austenite, which transforms first. The movement of high  $d_{111}$  peak to larger magnitudes, which is consistent with enrichment of the austenite with carbon partitioned from bainitic ferrite, respectively.

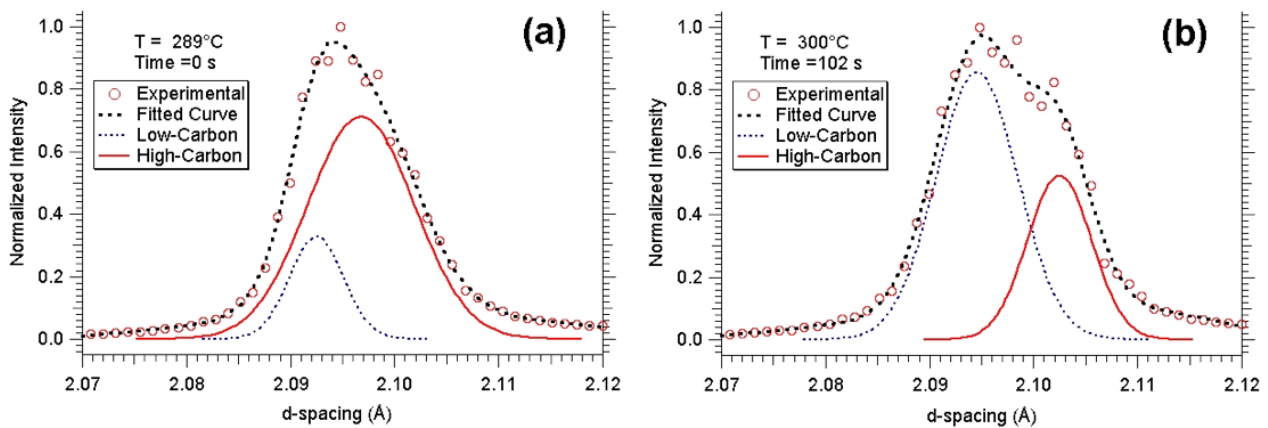


Fig. 3: FeCSiMn steel data analysis: Bimodal shape of austenite {111} diffraction peaks using two distinct austenite diffraction peaks with two different nominal  $d_{111}$  spacing.

### 3.2 Results from FeNi and FeNiC system

Similar austenite peak splitting and transformation of low- $d_{111}$  peak first was observed in a Fe-C-Al-Mn weld [5]. However, this observation was made during continuous cooling after weld solidification. The intention here was to replicate the above experiments in carbon-free and carbon-containing austenite, using FeNi and FeNiC alloys. The results for FeNi show that the {111} austenite diffraction peaks did not split, Fig. 4.

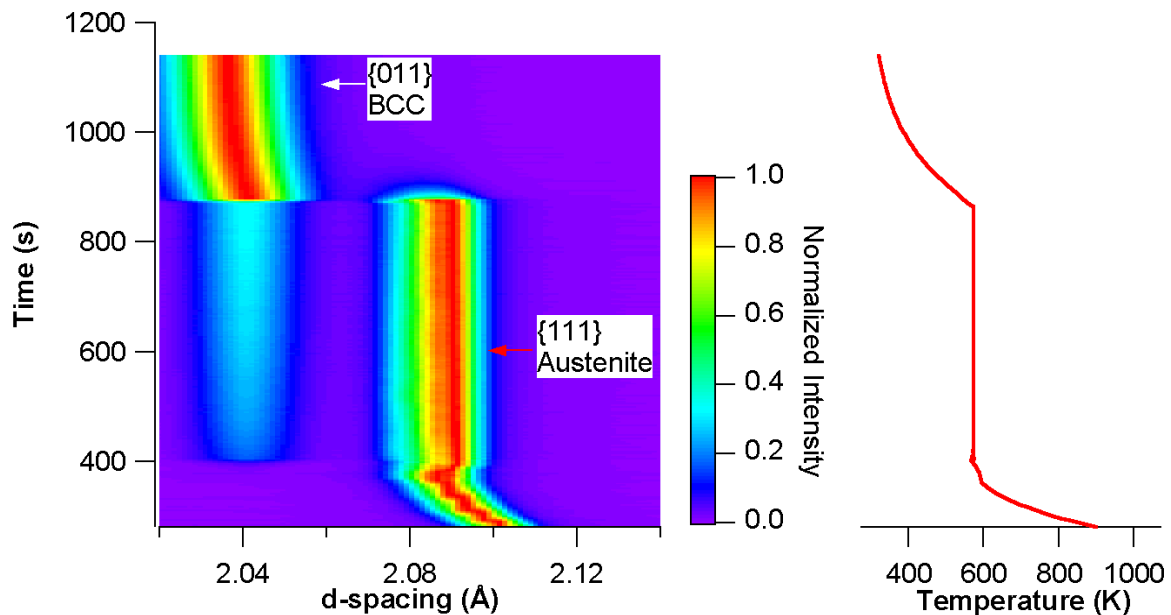


Fig.4 Image representation of TRXRD data from FeNi steel during cooling to 573 K, isothermal holding at 573K and while cooling from 573 K to room temperature. The plots also show the temperature variations as a function of time;

The austenite started to decompose at this temperature, as indicated by the appearance of BCC {011} peaks. The kinetics data [Fig. 5] show sudden transformation as soon as the sample reached 573 K, followed by a gradual increase in the BCC intensity during isothermal treatment. The remaining austenite decomposed rapidly on cooling to ambient temperature, Fig. 6, leaving no retained austenite. The optical microstructure revealed martensite lath with Vickers hardness  $317 \pm 5$  HV.

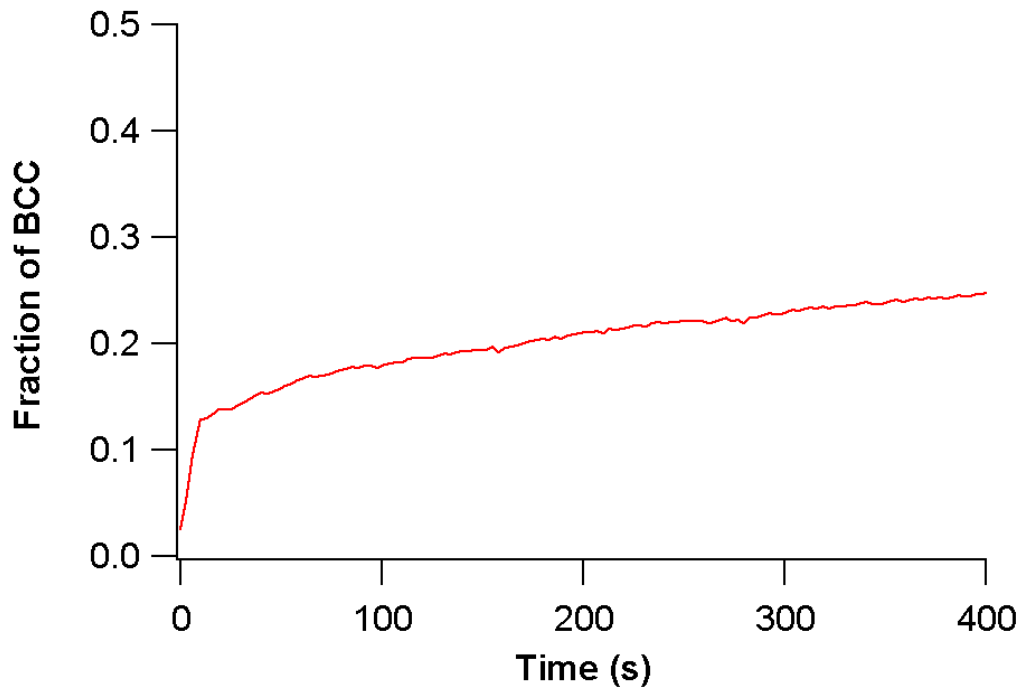


Fig. 5 Kinetics of martensite formation during isothermal hold at 573 K in Fe-Ni steel

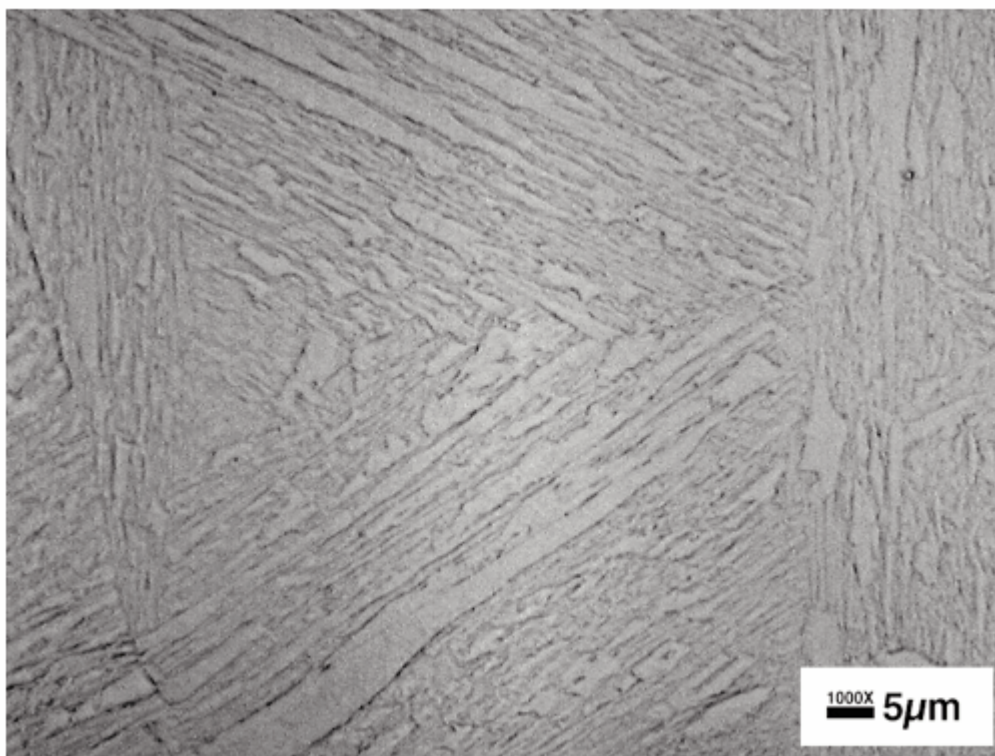


Fig. 6 Optical microstructure of the Fe-Ni steel after the heat-treatment

Fig. 7 shows the data from FeNiC – the {111}-austenite peak once again split on reaching 573 K but there was no evidence for BCC diffraction peaks throughout isothermal holding treatment. The experiment was repeated using another sample and again showed the peak splitting.

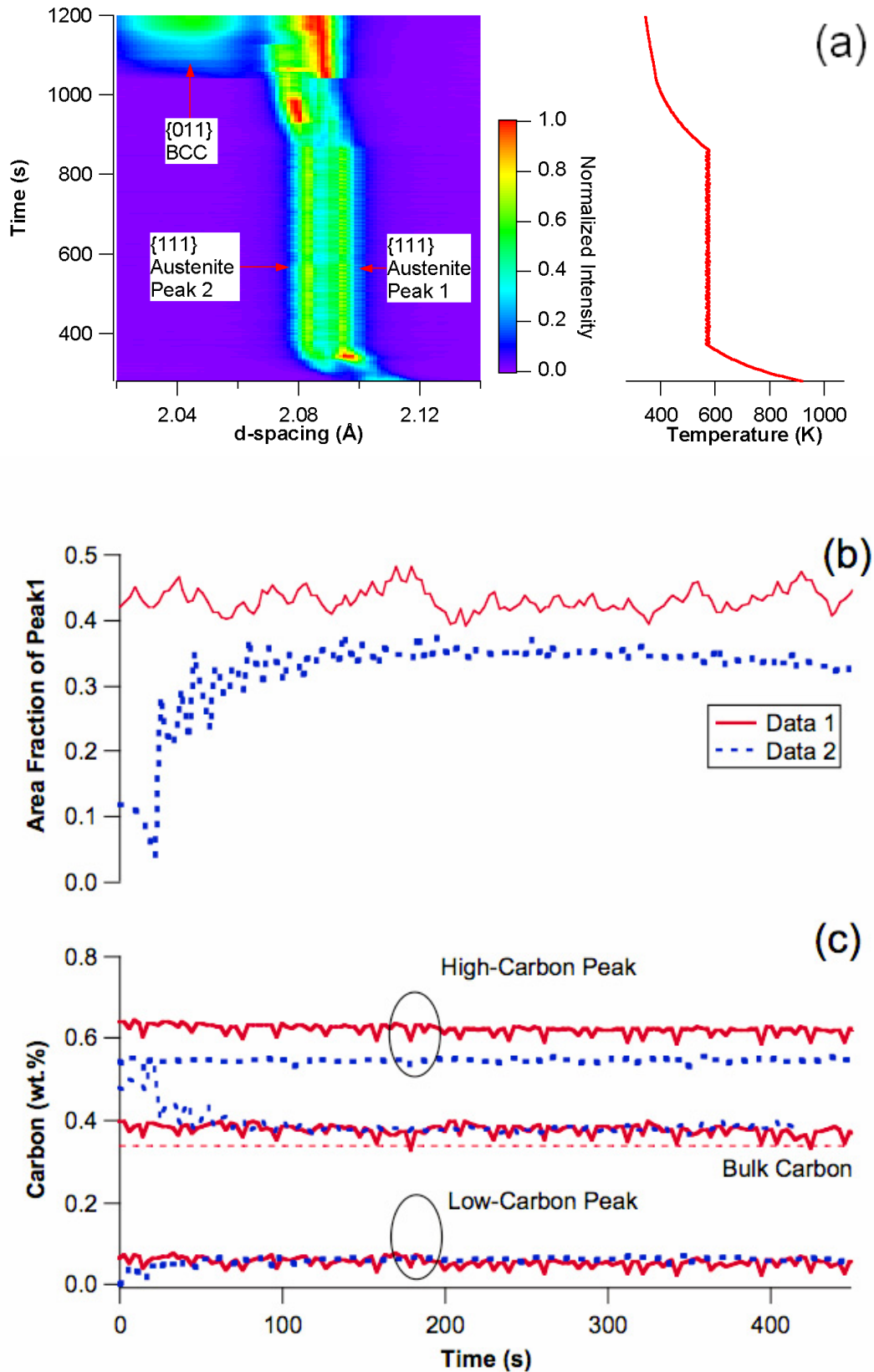


Fig. 7 X-ray data from (a) FeNiC during cooling to 573 K, isothermal holding at 573 K and while cooling from 573 K to room temperature. (b) Area fraction of peak 1 to peak 2 (c) Estimated of carbon concentrations of peak 1, peak 2 and bulk carbon based on the mass balance: The dotted line shows the bulk carbon concentration (0.35 wt.%) measured by traditional chemical analysis.



The data from two experiments are summarized in Fig. 7b. The ratio between low  $d_{111}$  peaks and high  $d_{111}$  peaks range from 0 to 0.5. These values are similar to the one measured from FeCSiMn steels. These results in particular indicate a role of carbon in causing the peak splitting, as speculated previously [4]. It is of interest to estimate the carbon concentration of these two austenite peaks. Using the published relationship (see equation 1) between the austenite composition and lattice parameter at room temperature (300 K) ( $a_{FCC}$ ), the carbon concentrations of these two austenite regions was estimated.

$$d_{\{111\}}^{FCC} = a_{FCC} / \sqrt{3}$$

$$a_{FCC} = 3.5780 + 0.033x_c + 0.00095x_{Mn} - 0.0002x_{Ni} + 0.0006x_{Cr} + 0.0056x_{Al} + 0.0031x_{Mo} + 0.0018x_V \quad (1)$$

In the above equation  $x_i$  corresponds to the weight percent of elements “ $i$ ” in the austenite. The variations of estimated carbon concentration of the two peaks, as well as, the estimated bulk carbon concentrations are shown Fig. 7c. The averages of these estimations are provided in Table 2. The calculations show the reproducibility of the experiments in terms of estimated bulk carbon concentrations in both experiments.

Table 2. Summary of carbon concentrations estimated from diffraction data:

Experiments	Low- $d_{111}$ Carbon (wt.%)	High- $d_{111}$ Carbon (wt.%)	Bulk Carbon (wt.%)
Data 1	$0.05 \pm 0.01$	$0.62 \pm 0.01$	$0.38 \pm 0.01$
Data 2	$0.06 \pm 0.01$	$0.55 \pm 0.01$	$0.39 \pm 0.03$

However, the bulk carbon concentration estimated from diffraction data is slightly higher than the value (0.34 wt.%) measured by standard chemical analysis techniques. Sensitivity analysis showed that the estimated bulk carbon concentration is very sensitive to the absolute position of the X-ray diffraction peaks. Small shifts in the peak location may change these estimated carbon concentrations. Therefore, the estimated carbon concentrations of peaks need to be confirmed with other characterization techniques. For example, the carbon concentration of the retained austenite in FeNiC steels can be measured by atom probe analysis and compared with estimated carbon concentration from X-ray diffraction data.

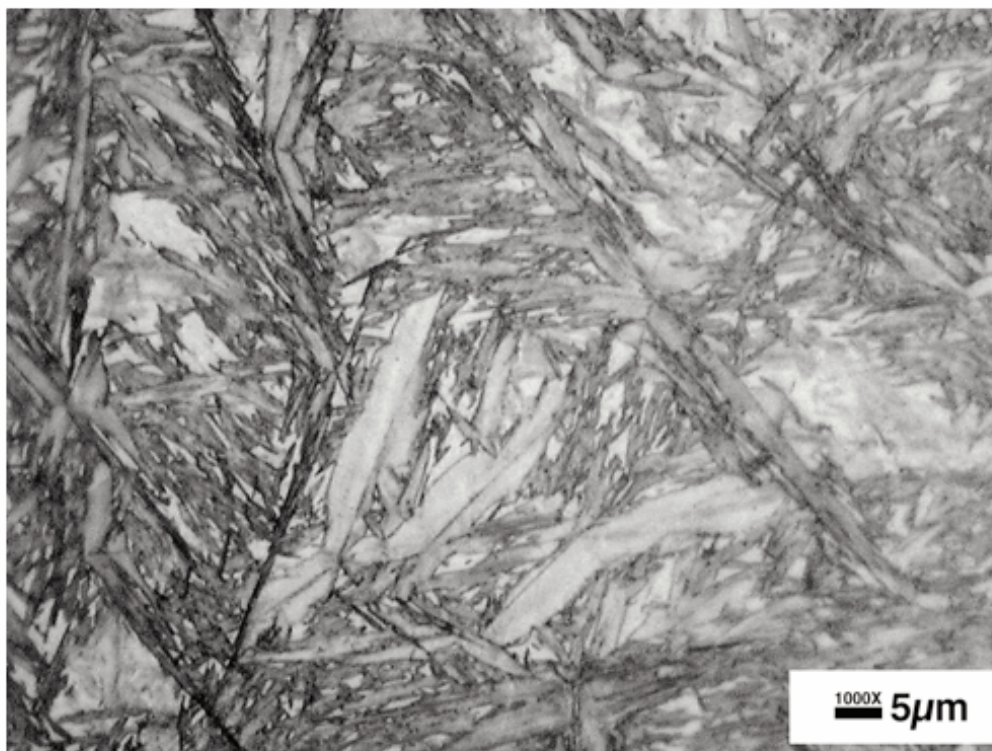


Fig. 8 Optical microstructure of the FeNiC steel showing martensite microstructure

The response on cooling from 573 K to room temperature on these FeNiC austenite peaks was found to be complex. There were unpredictable fluctuations in peak intensities together with the appearance of broad  $\{011\}$  BCC diffraction peaks had large effects on the austenite peak locations. Further work is necessary to understand these observations. The

retained austenite fraction was 0.27-0.35 at ambient temperature. Due to the large peak broadening, the tetragonality of the martensite could not be inferred from the current data. Optical microscopy (Fig. 8) confirmed the presence of lenticular martensite typical of FeNiC alloys. The hardness of this microstructure was 516±37 HV.

#### 4. DISCUSSION

The results from FeCSiMn and FeNiC steels showed austenite peak splitting while for the FeNi alloy did not. Possible mechanisms are briefly mentioned:

- Decarburization from surface: Decarburization from surface will lead to a gradual change in carbon concentration from the surface to certain depth. This would only lead to peak broadening and eventual movement of peak to low lattice parameter. The observed stable peak splitting is not consistent with decarburization from surface. In addition, optical microscopy and hardness measurements did not show any evidence for soft layer near the surface. Therefore, the observed peak splitting could not be attributed to the decarburization.
- Spatial Variation of Carbon: This could be interpreted as evidence for carbon somehow becoming heterogeneously distributed in the austenite, as has been speculated in the past [6]. However, our current knowledge of the thermodynamics of carbon in austenite does not support uphill diffusion.
- Strain in austenite: During the formation of plate shaped ferrite, the strains can be accommodated entirely in the austenite [7]. Moreover, this would be inconsistent with the observations on the FeNiC steel, which did not transform during peak splitting.
- Co-existence of high and low molar volume states of austenite at any temperature: The apparently large thermal expansivity of austenite is because the fraction of each state is temperature dependent [8]. Unfortunately, this does not involve time or carbon dependence.

The conclusion must therefore be that the role of carbon in austenite needs further study.

#### 5. SUMMARY

The most important outcome of the present work is the comparison between the FeNi and FeNiC austenite phases. The FeNiC austenite develops into regions with two lattice parameters whereas the formed does not. This indicates a role of carbon in the peak splitting phenomenon. The mechanism for such phenomenon any such effect is not obvious.

#### 7. ACKNOWLEDGMENTS

Research sponsored by the Division of Materials Sciences and Engineering, U. S. Department of Energy, under Contract DE-AC05-00OR22725 with UT-Battelle, LLC. The UNICAT facility at the Advanced Photon Source is supported by the U.S. DOE under Award No. DEFG02-91ER45439, through the Frederick Seitz Materials Research Laboratory at the University of Illinois at Urbana-Champaign, the Oak Ridge National Laboratory (U.S. DOE contract DE-AC05-00OR22725 with UT-Battelle LLC), the National Institute of Standards and Technology (U.S. Department of Commerce) and UOP LLC.

#### 8. REFERENCES

- [1] F. G. Caballero, H. K. D. H. Bhadeshia, K. J. A. Mawella, D. G. Jones and P. Brown: *Materials Science and Technology*, 17 (2001), 512
- [2] M. Peet, S. S. Babu, M. K. Miller and H. K. D. H. Bhadeshia, *Scripta Materialia*, 50 (2004), 1277
- [3] F. G. Caballero, M. K. Miller, S. S. Babu, C. Garcia-Mateo: *Acta Materialia* 55 (2007), 381
- [4] S. S. Babu, et al: *Metal. Mater. Trans. A* 36A (2005) 3281
- [5] S. S. Babu, J. W. Elmer, J. M. Vitek, and S. A. David: *Acta Materialia* 50 (2002), 4763
- [6] K. Tsuzaki, K. Fujiwara and T. Maki: *Materials Transactions, JIM*, 32(1991), 667
- [7] H. K. D. H. Bhadeshia, "Bainite in Steels," 2<sup>nd</sup> Edition, Institute of Materials, London, 2001
- [8] L. Kaufman, E.V. Clougherty, and R. J. Weiss, *Acta Metallurgica*, 11(1963) 323